Listeriolysin O Secreted by *Listeria monocytogenes* into the Host Cell Cytosol Is Degraded by the N-End Rule Pathway[▽]

Pamela Schnupf,[1]† Jianmin Zhou,[4] Alexander Varshavsky,[4] and Daniel A. Portnoy[1,2,3]*

Graduate Group in Microbiology,[1] Department of Molecular and Cellular Biology,[2] and School of Public Health,[3] University of California, Berkeley, California 94720-3202, and Division of Biology, California Institute of Technology, Pasadena, California 91125[4]

The intracellular pathogen *Listeria monocytogenes* escapes from a phagosomal compartment into the cytosol by secreting the pore-forming cytolysin listeriolysin O (LLO). During the proliferation of *L. monocytogenes* bacteria in the mammalian cell cytosol, the secreted LLO is targeted for degradation by the ubiquitin system. We report here that LLO is a substrate of the ubiquitin-dependent N-end rule pathway, which recognizes LLO through its N-terminal Lys residue. Specifically, we demonstrated by reverse-genetic and pharmacological methods that LLO was targeted for degradation by the N-end rule pathway in reticulocyte extracts and mouse NIH 3T3 cells and after its secretion by intracellular bacteria into the mouse cell cytosol. Replacing the N-terminal Lys of LLO with a stabilizing residue such as Val increased the in vivo half-life of LLO but did not strongly affect the intracellular growth or virulence of *L. monocytogenes*. Nevertheless, this replacement decreased the virulence of *L. monocytogenes* by nearly twofold, suggesting that a destabilizing N-terminal residue of LLO may stem from positive selection during the evolution of this and related bacteria. A double mutant strain of *L. monocytogenes* in which upregulated secretion of LLO was combined with a stabilizing N-terminal residue was severely toxic to infected mammalian cells, resulting in reduced intracellular growth of bacteria and an ~100-fold-lower level of virulence. In summary, we showed that LLO is degraded by the N-end rule pathway and that the degradation of LLO can reduce the toxicity of *L. monocytogenes* during infection, a property of LLO that may have been selected for its positive effects on fitness during the evolution of *L. monocytogenes*.

Listeria monocytogenes is a gram-positive, facultative, intracytosolic bacterial pathogen of humans and animals. In humans, *L. monocytogenes* infections are typically food borne and cause an invasive, sometimes fatal, disease in pregnant women, the elderly, newborns, and immunocompromised individuals (51, 66). Following internalization into mammalian cells, bacteria are initially contained within host vacuoles but rapidly escape into the cytosol, largely through the perforation of the phagosomal membrane by the pore-forming toxin called listeriolysin O (LLO) (46, 66). LLO is an essential virulence factor, as *hly*Δ bacteria, which lack LLO, fail to escape from the phagosomal compartment and are attenuated 10,000-fold in comparison to their wild-type counterparts in the murine model of listeriosis (20, 33, 45, 46). Once in the host cytosol, *L. monocytogenes* cells grow and divide, exploiting a host mechanism of actin-based motility to move within the cytosol and to spread from cell to cell through the formation of long plasma membrane extensions that are taken up by neighboring cells (18, 34, 61). LLO is also required for productive cell-to-cell spread because it facilitates the disruption of bacterium-containing double-membrane vesicles within the secondarily infected cells (23).

LLO is a member of a large family of toxins, called cholesterol-dependent cytolysins, that are secreted by gram-positive bacterial pathogens (1, 62). Secreted toxin monomers bind cholesterol-containing membranes, oligomerize, and thereafter insert themselves into the membranes, forming pores of up to 30 nm in diameter (62). While LLO is essential for phagosomal escape and cell-to-cell spread in most cell types, its membrane-perforating activity is potentially cytotoxic and must be tightly regulated in order for *L. monocytogenes* to remain in its intracellular replicative niche. Indeed, there is an inverse correlation between toxicity and virulence: the more toxic an *L. monocytogenes* strain is to an infected cell, the less virulent it is in terms of its ability to spread the infection (24). An inappropriately high level of activity of LLO in the host cytosol results in plasma membrane perforation and lysis of the host cell (16, 24, 25). The subsequent exposure of *L. monocytogenes* to the host's extracellular defenses, particularly neutrophils, leads to decreased virulence (24).

LLO activity is controlled by several posttranscriptional mechanisms that include an acidic pH optimum for LLO pore formation (25), translational regulation of LLO synthesis (52), and host-mediated degradation of LLO in the cytosol (53, 68). Together, these mechanisms functionally overlap to limit LLO activity during the growth of *L. monocytogenes* in the host cytosol. For example, double mutations in LLO that compromise both the acidic pH optimum and translational regulation cause much greater host cell toxicity than either mutation alone (24, 25, 52, 53). In addition, the host cell toxicity of LLO from *L. monocytogenes* mutants with upregulated LLO translation is greatly increased when the host 26S proteasome is

---

* Corresponding author. Mailing address: Department of Molecular and Cell Biology, University of California, Berkeley, CA 94720-3202. Phone: (510) 643-3925. Fax: (510) 643-6334. E-mail: portnoy@berkeley.edu.

† Present address: Unité de Pathogenie Microbienne Moléculaire, Institut Pasteur, 28 rue du Docteur Roux, 75724 Paris, France.

inhibited by pharmacological agents, a treatment that makes the normally short-lived LLO a longer-lived protein (16, 52, 53, 68). Surprisingly, however, the inhibition of the proteasome alone (in the absence of enhanced LLO synthesis) does not result in significantly increased cytotoxicity (53).

The secreted LLO is destroyed in the cytosol by the ubiquitin (Ub)-proteasome system (53), but specific features of LLO that cause it to be a system's target remained unknown. Protein substrates of the Ub system, which controls the levels of many intracellular proteins, are conjugated to Ub through the action of E1, E2, and E3 enzymes (28, 44, 63). The selectivity of ubiquitylation is mediated largely by E3, which recognizes a substrate's degradation signal (degron) (7, 22, 60). The E3 Ub ligases are an exceptionally large family, with more than 1,000 distinct E3s in mammals (4, 13). The term Ub ligase denotes either an E2-E3 holoenzyme or its E3 component. A ubiquitylated protein bears a covalently linked poly-Ub chain and is targeted for processive degradation by the 26S proteasome (27, 69).

An essential determinant of one class of degrons, called N-degrons, is a substrate's destabilizing N-terminal residue. The set of destabilizing residues in a given cell type yields a rule, called the N-end rule, which relates the in vivo half-life of a protein to the identity of its N-terminal residue (see Fig. 1) (29, 30, 37, 63, 64). In eukaryotes, the N-degron consists of three determinants: a destabilizing N-terminal residue of a protein substrate, its internal Lys (K) residue(s) (the site of formation of a poly-Ub chain), and a conformationally flexible region(s) in the vicinity of these determinants (7, 31, 47, 64). The N-end rule has a hierarchic structure in that some of the destabilizing N-terminal residues (Arg, Lys, His, Phe, Leu, Trp, Tyr, and Ile) are recognized directly by E3 Ub ligases of the N-end rule pathway, which are called N-recognins, whereas the other destabilizing N-terminal residues (Asn, Gln, Asp, Glu, and Cys) must be modified in vivo, enzymatically or otherwise, for their subsequent recognition by (functionally overlapping) N-recognins (see Fig. 1) (2, 29, 30, 36, 64). Physiological functions of the N-end rule pathway include its roles in the control of signaling by nitric oxide (NO) and G protein-coupled receptors, the regulation of peptide import and the fidelity of chromosome segregation, apoptosis, meiosis, cardiovascular development, neurogenesis, and pancreatic functions, as well as leaf senescence and the auxin transport and signaling in plants (references 29 and 30 and references therein).

Secreted LLO bears the N-terminal Lys residue, owing to the removal of the LLO's signal sequence by a bacterial signal peptidase during LLO secretion from *L. monocytogenes*. N-terminal Lys is a (primary) destabilizing residue in the N-end rule (see Fig. 1), suggesting that LLO may be a physiological substrate of the N-end rule pathway in the cytosol of infected mammalian cells. As shown in the present work, LLO is indeed an N-end rule substrate. We also found that replacing the N-terminal Lys of LLO with a stabilizing residue, such as Val, increased the in vivo half-life of LLO but did not strongly affect the intracellular growth or virulence of *L. monocytogenes*. Nevertheless, this replacement decreased the virulence of *L. monocytogenes* by nearly twofold, suggesting that a destabilizing N-terminal residue of LLO may stem from positive selection during the evolution of this and related bacteria. When long-lived (mutant) LLO proteins were also overproduced by

TABLE 1. Constructs and *L. monocytogenes* strains used for this study

| LLO protein[a] | LLO plasmid[b] | LLO plasmid *L. monocytogenes* strain in background: | |
		Δhly[c] (DP-L2161)	ΔactA Δhly (DP-L4813)
Wild type	DP-E4817	DP-L4818	DP-L4896
K25R	DP-E4861	DP-L4928	DP-L4882
K25G	DP-E4874	DP-L4929	DP-L4899
K25V	DP-E4875	DP-L4930	DP-L4900
K25L	DP-E4876	DP-L4931	DP-L4901
K25F	DP-E4995	DP-L4997	DP-L4996
K25A	DP-E4880	DP-L4933	DP-L4905
K25T	DP-E4879	DP-L4934	DP-L4903
S44S	DP-E4878	DP-L4966	
K25R S44S	DP-E4912	DP-L4967	
K25G S44S	DP-E4913	DP-L4968	
K25V S44S	DP-E4914	DP-L4969	
K25L S44S	DP-E4915	DP-L4970	
K25F S44S	DP-E4921	DP-L4971	
K25A S44S	DP-E4961	DP-L4978	
K25T S44S	DP-E4962	DP-L4979	

[a] Mutant proteins are identified by their mutations.
[b] DP-E numbers indicate pPL2-LLO constructs in *E. coli*.
[c] Reference 32.

L. monocytogenes (owing to a second mutation), the LLO-mediated toxicity was synergistically and greatly increased. In summary, the degradation of LLO by the N-end rule pathway during infection limits the toxicity of overproduced LLO and may have been selected for its positive effects on fitness during the evolution of *L. monocytogenes*.

MATERIALS AND METHODS

Bacterial strains, mammalian cell lines, and reagents. Bacterial strains used in this study are described in Table 1. All strains were derivatives of the streptomycin-resistant *L. monocytogenes* strain 10403S of serotype 1/2a (11). To construct LLO$_{WT}$ and LLO$_{K25X}$ mutant strains, the NodI/PstI fragment containing the LLO-encoding *hly* gene, including its promoter and the full-length 5′ and 3′ untranslated regions, was subcloned from pPL1 into the integration vector pPL2 (38). Changes to residue K25 were made by site-directed mutagenesis by using standard methods (6). The codon for the (wild-type) Lys residue, at position 1 of the secreted (signal sequence-lacking) LLO, was converted into codons for the following alternative residues: Arg (AGA), Gly (GGT), Val (GTT), Leu (TTA), Phe (TTT), Ala (GCA), and Thr (ACA). For each mutation, the most abundant *L. monocytogenes* codon, according to the codon usage table from the Kazusa Research Institute (http://www.kazusa.or.jp/codon/), was used. The constructs (verified by DNA sequencing) were introduced into *Escherichia coli* SM10 and conjugated into the *L. monocytogenes* Δhly strain DP-L2161 and the Δhly ΔactA strain DP-L4813 (Table 1). The resulting *L. monocytogenes* strains, containing single-copy integrated plasmids, were verified by PCR using the primer pairs PL102/PL95 and PL93/PL95 (38) and were maintained on selective antibiotic-brain heart infusion (BHI) plates. *L. monocytogenes* DP-L4813 was produced via allelic exchange by deleting codons encoding residues 7 to 633 of ActA in strain DP-L2161 by using the plasmid pDP-3076 (58). For mammalian cell infection experiments, *L. monocytogenes* strains were grown without agitation in slanted 15-ml conical tubes overnight at 30°C in BHI broth and washed twice in phosphate-buffered saline (PBS) before infection.

The mouse J774 macrophage cell line was grown at 37°C and 5% CO$_2$ in Dulbecco modified Eagle medium (DMEM) with a high glucose content (GIBCO/Invitrogen, Carlsbad, CA) and with 7.5% fetal bovine serum (FBS; GemCell, Woodland, CA) and 2 mM glutamine. Mouse L2 fibroblasts were grown as described previously (59). NIH 3T3 cells were grown in DMEM with a high glucose content and 7% FBS (HyClone, Logan, UT). All reagents were purchased from Sigma-Aldrich (St. Louis, MO) unless otherwise noted. The proteasome inhibitors *N*-acetyl-L-leucyl-L-leucyl-L-norleucine (LLnL) and MG132 were purchased from Calbiochem (San Diego, CA).

Plasmids encoding Ub-LLO fusions. The pcDNA3-^{f}DHFR-Ub^{R48}-X-LLO$^{1-417}$-Flag$_2$ plasmid constructs encoded the previously described (39, 60) ^{f}DHFR-Ub^{R48} moiety (Flag-tagged mouse dihydrofolate reductase [^{f}DHFR] followed by a mutant Ub moiety containing residue R48 [Ub^{R48}]) fused to the mature (signal sequence-lacking) LLO protein that also lacked its C-terminal (membrane-interacting) domain 4. In the plasmid designation, X denotes a junctional amino acid residue of the LLO moiety that becomes N terminal after cotranslational cleavage at the Ub-X junction. In these constructs, X was either Lys, a destabilizing N-terminal residue of the secreted wild-type LLO, or Gly, a stabilizing residue in the N-end rule. The plasmids were constructed using PCR by amplifying the sequence encoding residues 25 to 417 of LLO (LLO$^{25-417}$) from genomic DNA of *L. monocytogenes* and using the primers that made the resulting fragment to encode the Flag epitope as well. The following primers were used: JZ004 (forward primer for the sequence encoding LLO with residue K25 [LLO$_{K25}$]), 5′ ATT TCA *CCC GGG* AAG GAT GCA TCT GCA TTC AAT AAA GAA AAT TCA ATT TCA TCC 3′; JZ006 (forward primer for the sequence encoding LLO with the K25G mutation [LLO$_{K25G}$]), 5′ ATT TCA *CCC GGG* GGC GAT GCA TCT GCA TTC AAT AAA GAA AAT TCA ATT TCA TCC 3′; and JZ008 (reverse primer encoding Flag-tagged LLO$_{G417}$), 5′ ATT *TCT AGA* GCC GCT GCC GCT CTT GTC ATC GTC GTC CTT GTA GTC TCC ATC TGT ATA AGC TTT TGA AGT TGT TTC AAT ATA TTC TGA 3′ (restriction sites are italicized; the codons for the N-terminal residue of LLO and the Flag sequence are underlined). The PCR-produced DNA fragments were verified by sequencing and then digested with SmaI and XbaI and ligated into the SmaI/XbaI-cut plasmid pcDNA3-^{f}DHFR-Ub^{R48}-M-cMos (56), replacing the open reading frame encoding Met–Flag-tagged c-Mos. A second Flag-encoding sequence at the 3′ end of the resulting LLO construct was then added at the XbaI site. The plasmid pcDNA3-^{f}DHFR-Ub^{R48}-M-cMos^f was derived from pcDNA3-^{f}DHFR-Ub^{R48}-M-cMos (56) by introducing a Flag sequence after the XbaI site through PCR.

Assays with transcription-translation reticulocyte lysate. The TNT quick-coupled transcription-translation system (Promega, Madison, WI) was a rabbit reticulocyte lysate premixed with additional components necessary for carrying out transcription and translation in the lysate, including a mixture of amino acids other than Met. [^{35}S]methionine (>1,000 Ci/mmol; Amersham Pharmacia Biotech, Piscataway, NJ) was added to label newly synthesized proteins in reaction mixtures. Reactions were set up according to the manufacturer's instructions and were carried out at 30°C for 1 h, followed by the addition of 1 volume of 2× sample buffer (100 mM Tris-HCl, pH 6.8, 4% sodium dodecyl sulfate [SDS], 20% glycerol, 0.72 M β-mercaptoethanol, 0.1% bromophenol blue), heating at 95°C for 5 min, 10% SDS-polyacrylamide gel electrophoresis (PAGE), and autoradiography. Dipeptides were added to the final concentration of 1 mM. Stock solutions of dipeptides were 0.2 M in PBS containing 0.15 mM bestatin (Sigma).

Pulse-chase and Western analysis with LLO-transfected NIH 3T3 cells. Mouse NIH 3T3 cells grown to ~60% confluence were transfected with pcDNA3-Ub^{R48}-X-LLO$^{25-415}$-Flag$_2$ or with the control plasmid pcDNA3 or pcDNA3-^{f}DHFR-Ub^{R48}-R-nsP4 (56). For pulse-chase analysis, the medium was replaced with serum-free and methionine/cysteine-free DMEM after 16 h and cells were labeled for 10 min with ^{35}S protein-labeling mixture (PerkinElmer, Wellesley, MA) and then chased in DMEM with 10% FBS for 1 or 2 h. Cells were lysed in a mixture of 1% Triton X-100, 10% glycerol, 0.15 M NaCl, 5 mM Na-EDTA, and 20 mM Na-HEPES (pH 7.5) also containing 0.5 mM phenylmethylsulfonyl fluoride (PMSF) and protease inhibitor cocktail (Roche, Pleasanton, CA). The resulting extracts were clarified by centrifugation at 16,000 × g for 15 min, and samples of the supernatants (containing equal amounts of ^{35}S) were processed for immunoprecipitation with anti-Flag beads (Sigma). Immunoprecipitated proteins were fractionated using 10% SDS-PAGE, followed by autoradiography and quantitation with a PhosphorImager (Molecular Dynamics, Sunnyvale, CA). For Western blot analysis, cells were transfected for 24 h and then incubated with or without the proteasome inhibitor MG132 (50 μM) for 4 h. Next, cells were washed three times with PBS and then lysed in NP-40 lysis buffer (25 mM Tris [pH 7.5], 1 mM EDTA, 0.1 mM EGTA, 5 mM MgCl$_2$, 1% NP-40, 10% glycerol, 150 mM NaCl, 0.5 M PMSF, and 1× protease inhibitor cocktail [Roche, Mannheim, Germany]). The extracts were mixed with 2× sample buffer, boiled for 8 min, clarified by a 5-min spin at 16,000 × g, resolved on an 8% SDS-PAGE gel, transferred onto nitrocellulose, and then probed with polyclonal anti-LLO antibody.

N-terminal sequencing of secreted LLO proteins. *L. monocytogenes* strains secreting either LLO$_{K25R}$, LLO$_{K25V}$, or LLO$_{K25G}$ were grown to mid-logarithmic phase in Luria-Bertani (LB)-G1P medium (LB medium containing 25 mM glucose-1-phosphate, 5% activated charcoal, and 50 mM MOPS [morpholinepropanesulfonic acid], pH 7.4), and culture supernatants were precipitated with 10% trichloroacetic acid, washed with acetone, solubilized in SDS-sample buffer, and

fractionated using 4 to 12% gradient bis-Tris SDS-PAGE gels (NuPage; Invitrogen). Proteins were transferred onto polyvinylidene difluoride membranes by electroblotting in CAPS buffer {10% methanol–10 mM CAPS [3-(cyclohexylamino)-1-propanesulfonic acid] adjusted to pH 11 with NaOH} using a semidry gel blotter (Bio-Rad, Hercules, CA). Membranes were then stained with Coomassie blue, and the band corresponding to LLO was excised and processed for N-terminal sequencing (first three residues) at the Molecular Structure Facility (University of California, Davis).

Intracellular growth of *L. monocytogenes* in J774 macrophages and NIH 3T3 cells. Growth curves of *L. monocytogenes* were determined as previously described (46). Cells were infected at an effective multiplicity of infection of 0.1 (J774 macrophages) or 0.01 (NIH 3T3 cells). Gentamicin at 50 μg/ml was added at 1 h (J774 macrophages) or 1.5 h (NIH 3T3 cells) postinfection (p.i.) for the duration of the experiment. The proteasome inhibitor LLnL (20 μM) was added, when indicated, at 3 h p.i.

Pulse-chase analysis of LLO produced during intracellular growth of *L. monocytogenes*. The metabolic labeling of bacterial proteins with [^{35}S]methionine during the infection of J774 macrophages was based on the method of Moors et al. (41). J774 cells (2.2 × 10^6) were seeded onto 60-mm tissue culture dishes in DMEM and were infected the next day with an overnight (stationary-phase) culture of *L. monocytogenes* for 30 min at a multiplicity of infection of 1. Infected J774 cells were washed three times with PBS, after which DMEM and also, 30 min later, gentamicin (to 10 μg/ml) was added. At 4.5 h p.i., the medium was changed for 30 min to methionine-free (starvation) DMEM containing 2 mM Gln, 10% dialyzed FBS, 225 μg of cycloheximide/ml, and 30 μg of anisomycin/ml. Thereafter, cells were labeled for 1 h in 0.5 ml of the same medium with 0.2 mCi (per plate) of the ^{35}S protein-labeling mixture (PelkinElmer). In some experiments, the proteasome inhibitor LLnL was included at 50 μM in both starvation and labeling media. After 1 h, the labeling medium was replaced with chase medium (DMEM, 7.5% FBS, 2 mM Gln or 20 μg of chloramphenicol/ml, 5 mM Met). At the times indicated below, cell monolayers were washed three times with cold PBS and lysed by the addition of 1 ml of KD lysis buffer (2% Triton X-100, 0.02% saponin, 10 mM EDTA, PBS without Mg^{2+} or Ca^{2+}) containing protease inhibitors (1 mM PMSF, 0.3 μM aprotinin, 1 μM leupeptin, and 1 μM pepstatin A). Both bacteria and insoluble mammalian cell contents were removed by a 10-min spin at 16,000 × g. Supernatants were immunoprecipitated with anti-LLO monoclonal antibody B3-19 (43) as described previously (12). The immunoprecipitates were processed (see above) for 7.5% SDS-PAGE, autoradiography, and the quantitation of LLO bands with a Typhoon phosphorimager (Amersham Biosciences, Arlington Heights, IL) and ImageQuant software (Molecular Dynamics). To ensure equivalent levels of infection for all strains, three 12-mm coverslips per dish were included. The coverslips were removed at 4.5 h p.i. and were used to calculate the number of CFU per dish. In experiments that involved the dephosphorylation of immunoprecipitated LLO$_{K25G}$, 20 U of calf intestinal phosphatase (New England Biolabs, Beverly, MA) was employed as previously described (12).

Plaque formation in L2 fibroblasts. Plaque formation in mouse L2 fibroblasts was carried out as previously described (59), and plaques were scored by the method of Skoble et al. (58). Briefly, L2 fibroblasts grown to confluence in 6-well tissue culture plates were infected with 0.25 μl (per plate) of PBS-washed overnight cultures of *L. monocytogenes*. After 1 h, cell monolayers were washed three times with PBS and the medium was replaced with DMEM agar containing 40 μg of gentamicin/ml, the plates were incubated for 3 days, and plaques were visualized using an additional DMEM agar overlay containing 40 μg of gentamicin/ml and neutral red (GIBCO/Invitrogen) after incubation for 8 h. The relative plaque size is reported as a percentage of the wild-type plaque size.

Immunoblotting analysis of LLO. Overnight cultures of *L. monocytogenes* were diluted 20-fold in LB medium and incubated with shaking for 2.5 h at 37°C to mid-logarithmic phase (optical density at 600 nm [OD$_{600}$] of ~0.4). Bacteria were washed once with PBS and diluted into prewarmed LB medium to an OD$_{600}$ below 0.01. At various times postinoculation, 1-ml samples were removed for OD$_{600}$ measurements and LLO immunoblotting. The samples were centrifuged at 16,000 × g for 10 min, and the supernatants were removed and precipitated with 10% trichloroacetic acid, washed with acetone, and processed for SDS-PAGE as described above. Fractionated proteins were electroblotted onto nitrocellulose membranes, and LLO was detected using a rabbit polyclonal antibody to LLO (52), horseradish peroxidase-conjugated anti-rabbit immunoglobulin G (IgG) secondary antibody, and the ECL Plus Western blotting kit according to the instructions of the manufacturer (Promega). To quantitate band intensities, parallel samples were resolved by SDS-PAGE and subjected to the same procedure, except that the secondary antibody was Alexa Fluor goat anti-rabbit antibody (Invitrogen), followed by analysis with an Odyssey infrared imager (LI-COR Biosciences, Lincoln, NE).
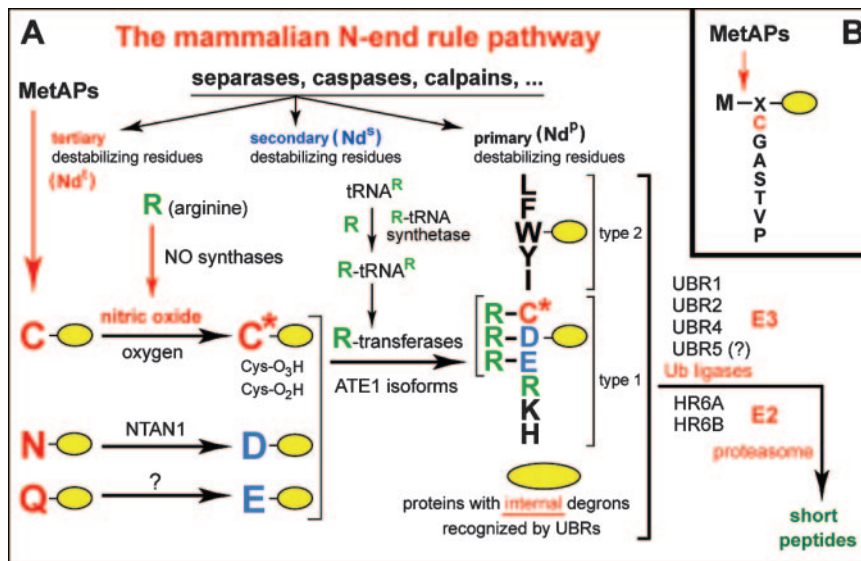
FIG. 1. Mammalian N-end rule pathway. (A) N-terminal residues are indicated by single-letter abbreviations for amino acids. The yellow ovals denote the rest of a protein substrate. C^* denotes oxidized N-terminal Cys, either Cys-sulfinic acid [$CysO_2(H)$] or Cys-sulfonic acid [$CysO_3(H)$], produced in reactions mediated by nitric oxide (NO) and oxygen (O_2) or oxygen derivatives, with subsequent arginylation of oxidized Cys by the *ATE1*-encoded isoforms of Arg-tRNA-protein transferase (R-transferase). (NO is produced from Arg by NO synthases.) The type 1 and type 2 primary destabilizing N-terminal residues are recognized by multiple E3 ubiquitin ligases (N-recognins) of the N-end rule pathway, including UBR1 and UBR2. Through their other substrate-binding sites, these E3s also recognize internal (non-N-terminal) degrons in other substrates of the N-end rule pathway, denoted by a larger oval. The dots after "calpains" refer to the expectation that physiologically relevant N-degrons can also be produced by intracellular proteases additional to those cited. MetAPs, methionine aminopeptidases; NTAN1, N-terminal asparagine-specific amidase; Nd^t, Nd^s, and Nd^p, tertiary, secondary, and primary N-terminal destabilizing residues, respectively. Modified from *Nature* (30) with permission of the publisher. (B) MetAPs remove Met from the N terminus of a polypeptide if the residue at position 2 belongs to the set of residues shown (64). Reprinted from *Nature* (30) with permission of the publisher.

Mouse infections. Cultures of *L. monocytogenes* strains encoding the LLO proteins indicated below were prepared in BHI medium as previously described and stored at −80°C (52). On the day of inoculation, the samples were thawed at room temperature and the strains were subcultured into BHI medium and grown to mid-logarithmic phase at 37°C with agitation. Bacterial cultures were washed once with PBS and diluted in PBS to 5×10^6 bacteria per ml. Samples containing 10^6 bacteria were injected into 7-week-old female BALB/c mice via the tail vein. Animals were sacrificed 24 h after inoculation. The livers and spleens were homogenized in 0.2% saponin, and the level of viable bacteria in each organ was determined by plating samples of homogenates onto LB plates. Competitive indices for wild-type 10403S *L. monocytogenes* versus Δ*hly* bacteria expressing LLO_{K25X} (where X is the N-terminal replacement residue) from an integrated plasmid harboring a chloramphenicol resistance gene were determined essentially as described in reference 5. In this assay, the *L. monocytogenes hly* deletion strain that was complemented with wild-type LLO (*L. monocytogenes* LLO_{WT}) had a minor virulence defect compared to 10403S. The ratios of bacteria of LLO_{K25X}-expressing strains to 10403S bacteria were determined by plating organ homogenates onto LB plates and then patching 100 colonies onto chloramphenicol (20-μg/ml)-containing plates. The 50% lethal dose (LD_{50}) of each *L. monocytogenes* strain for BALB/c mice was determined by Cerus Pharmaceuticals (Concord, CA) essentially as previously described (46) except that mice were injected with twofold dilutions and monitored for 7 days postinoculation.

RESULTS

LLO is a substrate of the N-end rule pathway. Mammalian reticulocytes (immature red blood cells) and their ATP-supplemented lysates contain an active Ub system including the N-end rule pathway (15, 26, 48). We asked whether LLO with the wild-type N-terminal residue Lys (Lys-LLO; derived from a Ub–Lys-LLO fusion) would be an N-end rule substrate in reticulocyte lysate. Our experiments utilized the Ub fusion technique (65), which makes it possible to engineer any protein to be expressed, in vivo or in vitro, as a Ub fusion whose (largely) cotranslational deubiquitylation yields a protein of interest with a desired N-terminal residue. The N-end rule pathway can be selectively inhibited in the lysate by the addition of dipeptides bearing either type 1 or type 2 destabilizing N-terminal residues. Through their interaction with, respectively, type 1 and type 2 substrate-binding sites of the ubiquitin-protein ligase E3 component N-recognin UBR1 and other N-recognins (see the introduction; also Fig. 1), such dipeptides act as specific competitive inhibitors of the N-end rule pathway (15, 26, 48). Since Lys, the N-terminal residue of wild-type LLO, is a type 1 primary destabilizing residue (Fig. 1), the degradation of Lys-LLO in reticulocyte lysate would be expected to be inhibited by a dipeptide such as, e.g., Arg-Ala, which bears a type 1 destabilizing N-terminal residue, but not by, e.g., Ala-Arg.

A transcription-translation reticulocyte lysate (see Materials and Methods) was used to express Lys-$LLO^{25–415}$ (Ub-Lys-$LLO^{25–415}$), which differed from wild-type LLO in lacking the C-terminal membrane-binding domain. These assays (Fig. 2A) utilized the previously developed Ub-protein-reference (UPR) technique, which increases the accuracy of such assays by providing a built-in reference protein (39, 60, 65). This method employs a linear fusion in which Ub is located between a protein of interest and a long-lived reference protein moiety, such as the mouse DHFR. The fusion is cotranslationally cleaved by Ub-specific deubiquitylating enzymes after the last
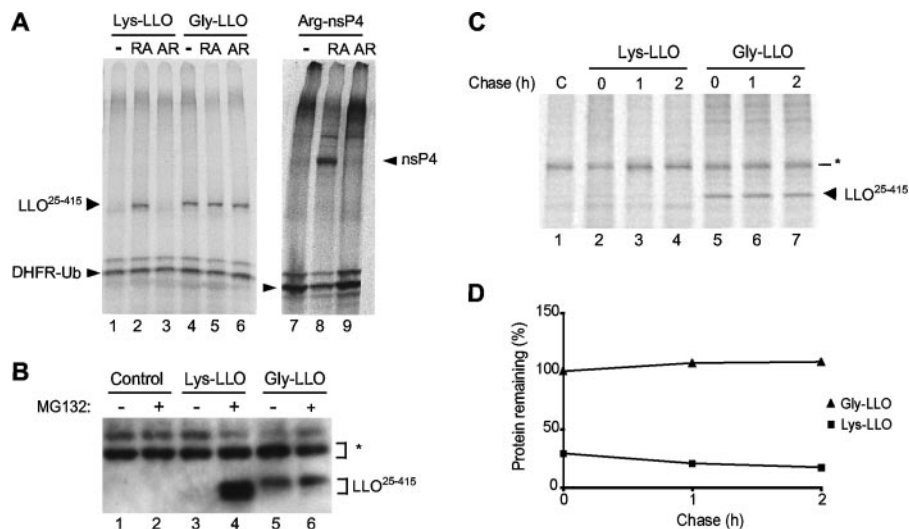
FIG. 2. LLO is a substrate of the N-end rule pathway. (A) A plasmid encoding the UPR technique-based fusion comprising ^{f}DHFR-Ub^{R48} and Flag-tagged Lys-LLO$^{25-415}$ (see Results) was expressed in a transcription-translation rabbit reticulocyte extract in the presence of [^{35}S]methionine for 1 h at 30°C, after which the extract was analyzed by SDS-PAGE and autoradiography. The above-mentioned fusion was cotranslationally processed into ^{f}DHFR-Ub^{R48} (a long-lived reference protein) and Flag-tagged Lys-LLO$^{25-415}$ (see Results). Lane 1, results of analysis in the absence of added dipeptides (−); lane 2, same as lane 1 but in the presence of 1 mM Arg-Ala (RA); lane 3, same as lane 1 but in the presence of 1 mM Ala-Arg (AR); lanes 4 to 6, same as lanes 1 to 3 but with Flag-tagged Gly-LLO$^{25-415}$; lanes 7 and 8, same as lanes 1 to 3 but with the control N-end rule substrate Arg-nsP4, a Sindbis virus RNA polymerase with a destabilizing N-terminal Arg (15, 56). (B) Stabilization of Flag-tagged Lys-LLO$^{25-415}$ in mouse NIH 3T3 cells by the inhibition of host proteasomes. The cells were transiently transfected with the plasmid pcDNA3 or plasmid constructs pcDNA3-Ub^{R48}-X-LLO$^{25-415}$-Flag$_2$ (where X represents Lys or Gly). After 24 h, cells were either left untreated (−; lanes 1, 3, and 5) or incubated with the proteasome inhibitor MG132 (50 μM) for 4 h (+; lanes 2, 4, and 6) before cells were lysed and the extracts were processed for Western blotting with polyclonal anti-LLO antibody. The asterisk (∗) indicates nonspecific bands that served as internal loading controls. (C) Degradation of Flag-tagged Lys-LLO$^{25-415}$ and Gly-LLO$^{25-415}$ in mouse NIH 3T3 cells. The cells were transiently transfected with pcDNA3-Ub^{R48}-X-LLO$^{25-415}$-Flag$_2$ plasmids. Cells were pulse-labeled with [^{35}S]methionine for 10 min and chased for 1 and 2 h, after which they were subjected to immunoprecipitation with anti-Flag antibody, SDS-PAGE, and autoradiography. Lane 1, vector alone (control [C]); lanes 2 to 4, cells expressing Flag-tagged Lys-LLO$^{25-415}$; lanes 5 to 7, cells expressing Flag-tagged Gly-LLO$^{25-415}$. (D) Quantification of the pulse-chase patterns in panel B, with the amount of Flag-tagged Gly-LLO$^{25-415}$ at the end of the pulse taken as 100%.

residue of Ub, producing equimolar amounts of the protein of interest and the reference protein bearing the C-terminal Ub moiety. The UPR technique can thus compensate for differences in protein yields and sample volumes and other sources of sample-to-sample variation (39, 65).

Using the previously described and validated steady-state assay with reticulocyte lysate (15), we determined the levels of ^{35}S-labeled synthesized Lys-LLO$^{25-415}$ in the lysate relative to the levels of the DHFR-Ub reference. In the presence of the Arg-Ala dipeptide, which bears a destabilizing N-terminal residue of the same (type 1) class as that of Lys-LLO (Fig. 1), the level of Lys-LLO$^{25-415}$ in the lysate was much higher than either in the presence of (compositionally identical) Ala-Arg or in the absence of added dipeptides (Fig. 2A, lanes 1 to 3). As expected, Phe-Ala, which contained a type 2 destabilizing N-terminal residue (Fig. 1), did not increase the levels of Lys-LLO$^{25-415}$ (data not shown), in contrast to Arg-Ala. This inhibitor-based evidence that ^{35}S-labeled Lys-LLO$^{25-415}$ in the lysate was targeted for degradation by the N-end rule pathway was independently supported by the results of an otherwise identical assay with Gly-LLO$^{25-415}$, which differed from Lys-LLO$^{25-415}$ solely by its N-terminal residue. (Gly is a stabilizing residue in the N-end rule [Fig. 1].) In contrast to those of Lys-LLO$^{25-415}$, the levels of ^{35}S-labeled Gly-LLO$^{25-415}$ produced in reticulocyte lysate were not altered by the addition of Arg-Ala, thus confirming, in a different way, that Lys-LLO$^{25-415}$

was degraded by the N-end rule pathway in reticulocyte lysate. The likely flexibility of LLO's N-terminal region, as evaluated by analogy with the similar perfringolysin O toxin of *Clostridium perfringens* (49) and the use of Phyre (http://www.sbg.bio .ic.ac.uk/phyre/) three-dimensional prediction software, presumably contributes to the targeting of Lys-LLO by the N-end rule pathway, given the previously established requirement for a flexible region downstream of a substrate's destabilizing N-terminal residue as one determinant of the substrate's N-degron (see the introduction).

To verify that Lys-LLO$^{25-415}$ was degraded by the N-end rule pathway in vivo as well, mouse NIH 3T3 cells were transiently transfected with plasmids that expressed either Lys-LLO$^{25-415}$ or Gly-LLO$^{25-415}$, the latter bearing a stabilizing N-terminal residue, with both test proteins produced by deubiquitylation of their Ub fusions (see above). We analyzed LLO degradation in NIH 3T3 cells by using both immunoblotting and pulse-chase assays. In the pulse-chase assays, the band of Gly-LLO$^{25-415}$ was prominent at the end of the 10-min pulse and remained undiminished throughout a 2-h chase, whereas the band of Lys-LLO$^{25-415}$ was barely detectable (at the same level of autoradiographic exposure) even before the chase, i.e., at the end of the 10-min pulse (Fig. 2C, lanes 2 to 4; compare lanes 5 to 7). While longer exposures than that for the sample shown in Fig. 2C allowed the detection of the band of pulse-labeled Lys-LLO$^{25-415}$, the quantitation of the band patterns con-

firmed the much lower level of pulse-labeled Lys-LLO$^{25-415}$ than of Gly-LLO$^{25-415}$ in NIH 3T3 cells, indicating the rapid degradation of Lys-LLO$^{25-415}$ during the 10-min pulse, i.e., even before the chase (Fig. 2D and data not shown). Interestingly, whereas young (pulse-labeled) molecules of Lys-LLO$^{25-415}$ were rapidly degraded by the N-end rule pathway in vivo, those (relatively few) molecules of Lys-LLO$^{25-415}$ that escaped degradation shortly after their synthesis were degraded at later times (during the chase) apparently at a much lower rate than their newly formed (young) counterparts (Fig. 2D). In other words, the activity of the N-degron of Lys-LLO$^{25-415}$ apparently decreased as a function of time posttranslation. This effect, previously observed with other N-end rule substrates (and substrates of other Ub-dependent pathways as well) is likely to stem, at least in part, from conformational changes (conformational maturation) that newly formed proteins undergo soon after their synthesis, including, for oligomeric proteins, the formation of either homo- or hetero-oligomers (9, 60).

Without proteasome inhibitors, Lys-LLO$^{25-415}$ was undetectable by immunoblotting, whereas Gly-LLO$^{25-415}$ was readily detectable (Fig. 2B, lanes 3 and 5). In striking contrast, the level of Lys-LLO$^{25-415}$ was greatly increased in NIH 3T3 cells after 4 h of treatment with MG132, a proteasome inhibitor, whereas the same treatment only marginally increased the level Gly-LLO$^{25-415}$ (Fig. 2B, lanes 3 to 6). Taken together, the above-cited in vitro (Fig. 1) and in vivo (Fig. 2) evidence identified Lys-LLO$^{25-415}$ as a substrate of the mammalian N-end rule pathway. These data also suggest that LLO may contain at least one other, apparently weaker, degron that is targeted by a non-N-end rule pathway.

***L. monocytogenes* strains secreting LLOs with different N-terminal residues.** To examine whether secreted LLOs bearing either destabilizing or stabilizing N-terminal residues (Fig. 1) would exhibit different functional properties and result in bacteria with different abilities to infect (and grow in) mammalian hosts, we began by constructing *L. monocytogenes* strains that secreted X-LLOs, in which X was either Gly or Val (stabilizing residues in the N-end rule), Arg (a type 1 destabilizing residue), Leu or Phe (type 2 destabilizing residues), Ala, or Thr. The latter two N-terminal residues, and Ser as well, can be destabilizing under certain conditions (26), but the corresponding N-recognin, i.e., an E3 Ub ligase(s) specific for N-terminal Ala, Thr, and Ser, has not been identified. In addition, N-terminal Ala, Thr, and Ser residues are often acetylated in vivo, a modification that would be expected to preclude their recognition as destabilizing residues.

LLO$_{K25R}$, LLO$_{K25V}$, and LLO$_{K25G}$ that were secreted by the corresponding *L. monocytogenes* strains were isolated to determine their N-terminal residues by Edman sequencing (see Materials and Methods). These tests directly confirmed the presence of Arg, Val, and Gly, respectively, at the N termini of the above-listed (mutant) X-LLO proteins, indicating that the residues that replaced wild-type Lys-25 did not alter the signal sequence cleavage site of LLO.

Previous work has shown that the 5′ untranslated region and the 5′-proximal part of the LLO-encoding *hly* mRNA are involved in regulating LLO synthesis during growth in vitro and in mammalian cells as well (52, 55). In particular, a single-codon change at residue Ser-44 of LLO that retained Ser as the

encoded residue strongly increased LLO production, resulting in host cell toxicity and intracellular growth and virulence defects (24, 52, 53). To determine whether the above-described alterations of the N-terminal residue of secreted LLO affect LLO synthesis, we assayed the relative amounts of mutant LLO$_{K25X}$ proteins that were produced during the in vitro growth of the corresponding *L. monocytogenes* strains. These tests included the LLO$_{S44S}$ *L. monocytogenes* mutant that produces a wild-type LLO but exhibits increased translation of the LLO mRNA during logarithmic growth (52).

The mutant *L. monocytogenes* strains grew indistinguishably from wild-type *L. monocytogenes* in both LB and BHI broth (Fig. 3A and data not shown). The relative levels of secreted LLO$_{K25X}$ proteins (determined by immunoblotting) were similar for all of the tested strains at the late stationary phase of growth in LB broth (Fig. 3B). In addition, all of the mutant LLO$_{K25X}$ proteins had activities similar to those of pore-forming proteins, as determined by assaying their abilities to lyse red blood cells (Fig. 3C). Furthermore, the alterations of the N-terminal residues in LLO$_{K25X}$ proteins did not affect the pH optimum of LLO (Table 2). There were small differences in the amounts of secreted LLO$_{K25X}$ proteins during exponential in vitro growth, although all of the observed differences were much below the ~9-fold overproduction of LLO by the LLO$_{S44S}$ *L. monocytogenes* mutant (Fig. 3B). Since the secreted LLO is not degraded in the medium during the in vitro growth of *L. monocytogenes* (52), the various levels of LLO$_{K25X}$ proteins produced by exponentially growing cells were most likely due to (relatively small) alterations in the rate of LLO synthesis. Thus, the mutational alterations of the N-terminal residue of the secreted LLO resulted in (at most) minor changes in the rate of its production and did not alter the pore-forming activity of LLO (Fig. 3 and Table 2).

Stabilization of LLO against degradation by the N-end rule pathway has minor effects on the intracellular growth or virulence of *L. monocytogenes*. We next examined the ability of the above-mentioned *L. monocytogenes* mutants to grow intracellularly in mammalian cells. The rates of growth of the *L. monocytogenes* LLO$_{K25X}$ mutants in mouse J774 macrophage-like cells for the first 8 h were lower than the rate of growth of the wild-type strain by up to twofold (Fig. 4A). By 11 h p.i., the strains expressing LLO$_{K25G}$, LLO$_{K25V}$, LLO$_{K25A}$, and LLO$_{K25T}$ exhibited a retardation of growth of up to fourfold in J774 cells (Fig. 4A). The strains expressing LLO$_{K25R}$, LLO$_{K25L}$, and LLO$_{K25F}$ (in which the wild-type destabilizing Lys residue was changed to another destabilizing residue) continued to exhibit at most twofold-slower growth than wild-type *L. monocytogenes* (Fig. 4A). However, none of the above-listed LLO mutants had a substantial growth defect in NIH 3T3 fibroblasts (Fig. 4B) or in the (3-day) plaque formation assay, which integrates both the intracellular growth of *L. monocytogenes* and its ability to infect neighboring cells (Fig. 4C). In contrast, *L. monocytogenes* LLO$_{S44S}$, which expresses strongly increased levels of LLO, exhibited a ~50-fold reduction in intracellular growth in J774 cells by 8 h p.i. and was unable to form plaques in L2 cell monolayers (52). Finally, we found that the *L. monocytogenes* LLO$_{K25X}$ mutants exhibited close to wild-type levels of virulence as measured by the LD$_{50}$s for BALB/c mice (Table 2), although minor virulence defects (up to a 1.9-fold reduction) in the liver were detected for the *L.*
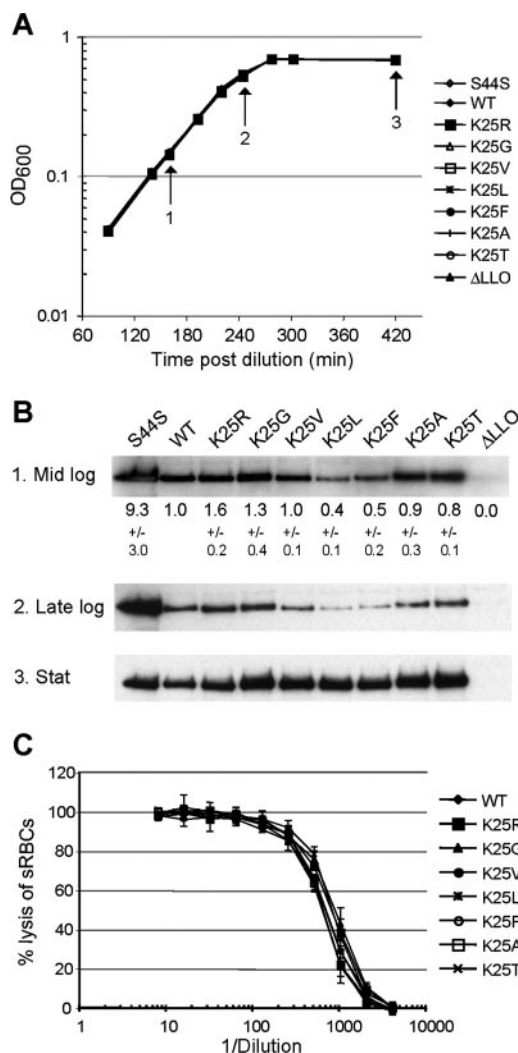
FIG. 3. Secretion of LLO bearing different N-terminal residues by *L. monocytogenes* strains growing outside host cells. (A and B) Growth (A) and LLO secretion (B) in LB medium by *L. monocytogenes* strains that produced either wild-type (WT) Lys-LLO or its derivatives containing other (indicated) N-terminal residues. The relative amounts of secreted X-LLO proteins (in mid-logarithmic [mid log], late-logarithmic [late log], and stationary [stat] phases of growth) were compared by immunoblotting. Shown are the results of one of five independent experiments. The numbers below the first row in panel B (which include standard deviations) refer to the quantitation of immunoblots from three samples taken during mid-exponential growth and analyzed with an Odyssey infrared imager. (C) Hemolytic activity of LLO present in stationary-phase culture supernatants from the *L. monocytogenes* strains with the indicated mutations. Error bars indicate standard deviations for three replicates in one experiment that is representative of four independent experiments. sRBCs, sheep red blood cells.

monocytogenes LLO$_{K25V}$ strain relative to *L. monocytogenes* LLO$_{WT}$ when the strains were directly compared to wild-type *L. monocytogenes* 10403S in the competitive index assay (see Fig. 7B and Discussion). Taken together, these results indicate that while the metabolic stabilization of secreted X-LLO detectably compromised the intracellular growth, cell-to-cell spread, and virulence of *L. monocytogenes*, the effects observed were relatively small (Fig. 3 and 4 and Table 2).

The identity of LLO's N-terminal residue affects LLO degradation in mammalian cytosol. LLO secreted from *L. monocytogenes* into the host cell cytosol becomes phosphorylated and ubiquitylated before its rapid, proteasome-dependent degradation (53). However, LLO secreted during cell-to-cell spread appears to be proteolytically cleaved but is otherwise longer lived, suggesting the existence of metabolically distinct subpopulations of LLO (53). To confine the analysis to LLO that is degraded in vivo, we introduced the wild-type and LLO$_{K25X}$ mutant alleles into an *L. monocytogenes* strain with a deletion of *actA*. The *actA* gene encodes a bacterial protein required for actin polymerization and the intercellular dissemination of *L. monocytogenes* (18, 34, 61). The absence of cell-to-cell spread did not result in a detectable effect on the intracellular growth of *L. monocytogenes* strains that secreted either LLO$_{WT}$ or LLO$_{K25X}$ by up to 8 h p.i. (data not shown).

Using pulse-chase analysis, we found that changing the N terminus of LLO from Lys to Arg, another type 1 primary destabilizing residue (Fig. 1), did not significantly affect the rate of LLO degradation (Fig. 5A). In contrast, the placement of other residues, including stabilizing residues, at the LLO N terminus led to a strong, up to 10-fold, metabolic stabilization of X-LLO (Fig. 5A). Stabilized X-LLO migrated as both a 58-kDa band (a species that comigrates with the full-length LLO minus the signal sequence) and a 60-kDa band. The latter, in the case of wild-type LLO, was previously shown to be its phosphorylated derivative (52). In agreement with this conclusion, phosphatase treatment shifted the 60-kDa species of immunoprecipitated LLO$_{K25G}$ to the 58-kDa form (Fig. 5B). In addition, larger (>60-kDa) LLO-containing species, which were previously shown to be ubiquitylated derivatives of LLO (53), were also observed (Fig. 5).

For reasons unknown, the replacement of a type 1 destabilizing residue such as Lys by a type 2 destabilizing residue such as Phe or Leu at the N terminus of LLO significantly stabilized the resulting X-LLO during the chase (Fig. 5A). However, the initial (postpulse) levels of Phe-LLO and Leu-LLO were lower than those of their counterparts in the case of, for example, Thr-LLO and Gly-LLO (Fig. 5A). These data are in agreement

TABLE 2. Hemolytic activity ratios and LD$_{50}$s of *L. monocytogenes* LLO strains

Strain[a]	Hemolytic activity ratio (dilution at pH 5.5/dilution at pH 7.4)[b]	LD$_{50}$[c]
Wild type	9.5	4.2×10^4
K25R	9.7	4.8×10^4
K25G	11.3	5.3×10^4
K25V	10.5	4.7×10^4
K25L	11.1	UD
K25F	11.9	3.5×10^4
K25A	11.3	3.7×10^4
K25T	11.5	UD

[a] Mutant strains are identified by the mutations in their LLOs.
[b] Ratio of the dilutions of supernatants from *L. monocytogenes* strains grown in LB broth to late stationary phase required for 50% lysis of sheep red blood cells when assayed at pH 5.5 and 7.4.
[c] The LD$_{50}$s were determined by injecting 6-week-old female BALB/c mice with twofold dilutions via the tail vein and monitoring the mice for 7 days. UD, undetermined.
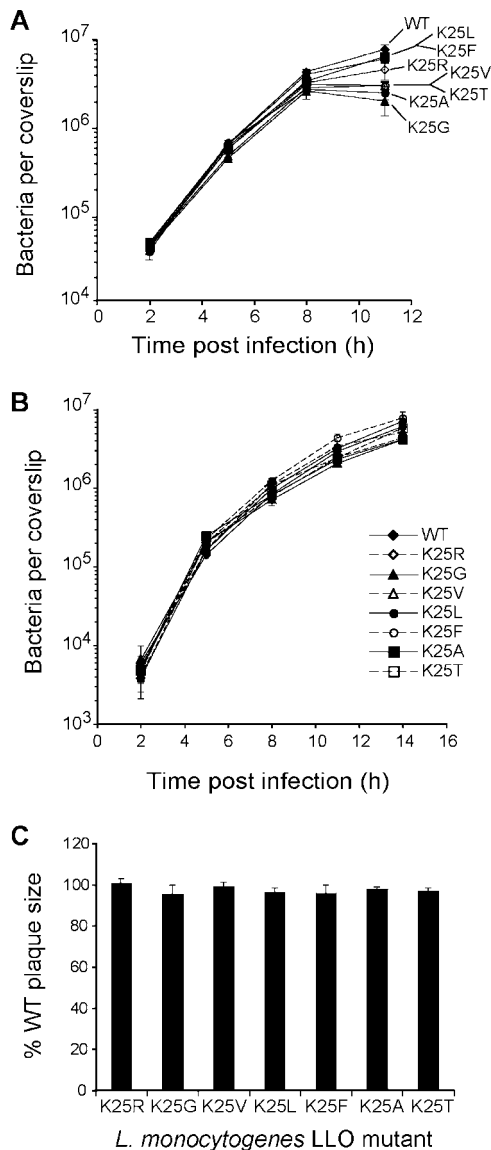
FIG. 4. Alterations of LLO's N-terminal residue have at most weak effects on the intracellular growth of *L. monocytogenes*. (A and B) Growth curves of *L. monocytogenes* LLO$_{WT}$ (WT; expressing Lys-LLO) and LLO$_{K25X}$ mutants (identified by the corresponding mutations) in J774 macrophages (A) and NIH 3T3 fibroblasts (B) (see Materials and Methods). Shown here are the results, including standard deviations, of one of at least three independent experiments with triplicate coverslips for each experiment. The *P* values for the growth difference between the LLO$_{WT}$ and LLO$_{K25X}$ strains of *L. monocytogenes* were 0.008 and 0.035 at 8 and 11 h p.i., respectively (based on Student's *t* test for one sample; http://www.statpages.org). (C) Sizes of plaques formed in mouse L2 fibroblasts by *L. monocytogenes* strains that produced the indicated X-LLO proteins relative to the size of plaques formed by the wild-type strain expressing Lys-LLO, which was set as 100%. Standard deviations were compiled from the results of three independent experiments.
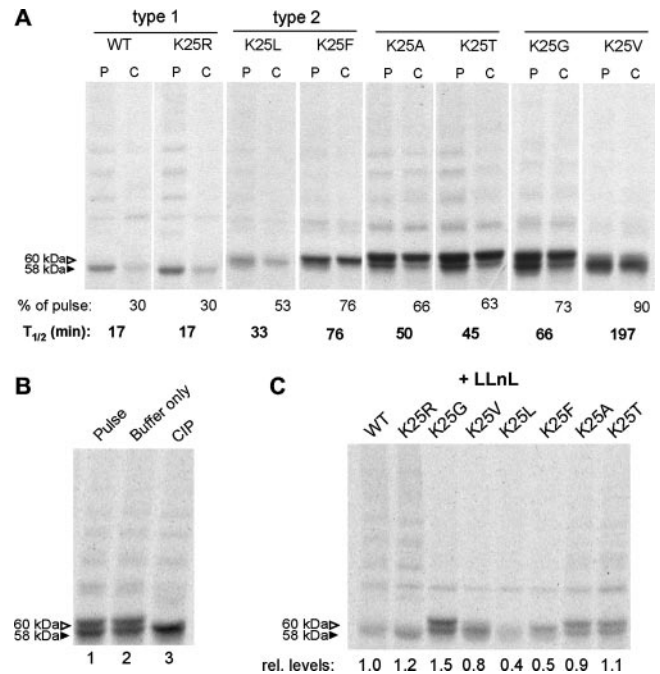

FIG. 5. Alterations of LLO's N-terminal residue affect its degradation in the host cell cytosol. (A) Pulse-chase analysis of X-LLO proteins (where X is Lys [wild type], Arg, Leu, Phe, Ala, Thr, Gly, or Val). X-LLOs were immunoprecipitated from extracts of J774 macrophages that were infected with nonspreading (*actAΔ*) *L. monocytogenes* strains secreting the indicated X-LLO proteins. P and C in panel A refer to pulse and chase, respectively. Cells were labeled at 5 h p.i. for 1 h with [^{35}S]methionine and, when indicated, chased for 30 min, after which they were subjected to immunoprecipitation with anti-LLO antibody, SDS-PAGE, and quantitation (see Materials and Methods). The band intensities after the chase, relative to those immediately after the pulse, were used to estimate the approximate half-lives ($T_{1/2}$) of X-LLO proteins. Shown are the results from one of two independent experiments. WT, wild type. (B) Immunoprecipitated LLO$_{K25G}$ (Gly-LLO; lane 1) was incubated either with buffer only (lane 2) or with buffer containing calf intestinal phosphatase (CIP; lane 3) for 20 h at 37°C prior to SDS-PAGE (lane 3). (C) X-LLOs with the indicated mutations were labeled with [^{35}S]methionine at 5 h p.i. for 30 min in the presence (+) of LLnL (see Materials and Methods). rel. levels, relative levels.

with the observed decrease in LLO production during the in vitro growth of *L. monocytogenes*, i.e., in the absence of host cells (Fig. 3B). Indeed, when the degradation of secreted X-LLO in the mouse cell cytosol was inhibited, during pulse-labeling, by the proteasome inhibitor LLnL, the relative levels

of pulse-labeled X-LLOs closely corresponded to those observed during the exponential growth of *L. monocytogenes* in the absence of host cells (Fig. 5C and 3B). Taken together, the patterns of X-LLO degradation in reticulocyte extract and in mouse NIH 3T3 cells (Fig. 2), as well as the degradation patterns of secreted X-LLO in the host cytosol (Fig. 5A), were a (qualitatively) self-consistent set, demonstrating directly that wild-type LLO, bearing N-terminal Lys, is a physiological substrate of the N-end rule pathway.

Synergistic impairment of intracellular growth of *L. monocytogenes* by a combination of overproduction and metabolic stabilization of LLO. Our previous work has shown that a higher rate of LLO production is synergistically cytotoxic with the metabolic stabilization of LLO, the latter achieved by the pharmacological inhibition of the proteasome (24, 52, 53). Specifically, treatment with a proteasome inhibitor has negligible effects on the intracellular growth of wild-type *L. monocytogenes*, but the same treatment results in high LLO-medi-
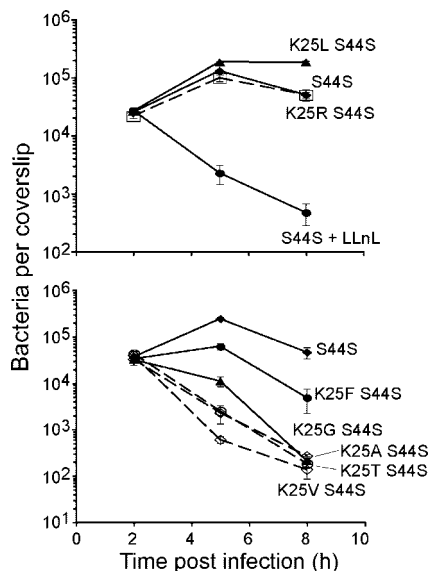
FIG. 6. Synergistic effects of both overproducing LLO and increasing its in vivo half-life on the intracellular growth of *L. monocytogenes* in mouse cells. Graphs depict the intracellular growth, in J774 macrophages, of *L. monocytogenes* strains that overproduced LLO (owing to the LLO_{S44S} mutation) and, when indicated, also contained mutational alterations of the N-terminal residue of LLO (K25X). See Materials and Methods for technical details. Error bars indicate standard deviations of results for triplicate coverslips from one experiment representative of three independent experiments.

ated toxicity when combined with mutations that increase the rate of LLO synthesis and secretion (52, 53). These results suggested that the proteasomal degradation of LLO becomes critical for intracellular growth when LLO is synthesized at higher-than-wild-type levels. To address these issues by stabilizing X-LLO through changes of its N-terminal residue (instead of a much less specific, metabolically pleiotropic inhibition of the proteasome), we constructed a panel of *L. monocytogenes* strains that combined alterations of the N-terminal residue of secreted LLO with the synonymous codon change at residue S44 that increases the rate of LLO production and secretion into the host cytosol at the level of LLO translation during cytosolic growth (52).

The analysis of the resulting double mutant bacteria revealed strikingly high levels of X-LLO toxicity (up to a 100-fold reduction in growth over 8 h p.i) when the S44S mutation was combined with a stabilizing N-terminal residue (Fig. 6). Through visual monitoring of the infection, it was clear that the observed synergistic growth defect of the K25X-S44S double mutants stemmed, in a large part, from their toxicity to the infected host cell (data not shown). Under the conditions of our assay, this toxicity was manifested as an increase in plasma membrane permeability. The increased permeability reduced the number of CFU through the influx of the bactericidal antibiotic gentamicin from the medium into the host cell, the lysis of the host cell, and the subsequent exposure of the bacteria to gentamicin in the medium. When a change of the N-terminal residue of LLO reduced the production of LLO both in vitro (in the absence of host cells) and during intracellular growth (Fig. 3B and 5C), the degree of synergism between a (partially)

stabilizing N-terminal alteration and the S44S mutation was also reduced (K25F and S44S) or lacking altogether (K25L and S44S) (Fig. 6). We conclude that LLO-mediated toxicity depends on the rates of both the production and degradation of LLO.

To explore further the effects of LLO degradation by the N-end rule pathway on the virulence of *L. monocytogenes*, we analyzed the S44S mutant and the K25X-S44S double mutants in the murine model of listeriosis (Fig. 7A and Materials and Methods). Strikingly, the levels of CFU of each *L. monocytogenes* mutant recovered from the spleens of infected mice strongly correlated with the observed growth defects of the corresponding mutant in the J774 macrophage cell culture model. Specifically, the replacement of the (wild-type) N-terminal Lys residue of LLO by stabilizing residues strongly increased the virulence defect of *L. monocytogenes* LLO_{S44S} in BALB/c mice, up to 100-fold after 24 h p.i. (Fig. 1, 6, and 7A). A similar pattern in the livers of infected mice was observed (Fig. 7A). While an effect of metabolically stabilized LLO_{K25V} on the virulence of the corresponding single-mutant strain appeared to be lacking when measured by the LD_{50} for BALB/c mice (Table 2), an up to nearly twofold decrease in virulence in the liver could be reproducibly detected using the competitive index assay (Fig. 7B) and is briefly considered below.

DISCUSSION

LLO that is secreted into the host cell cytosol during the intracellular growth of *L. monocytogenes* is phosphorylated, ubiquitylated, and rapidly degraded by the Ub-proteasome system (53, 68). In this study, we employed reverse-genetic and pharmacological techniques to directly demonstrate that secreted LLO, which bears N-terminal Lys, a type 1 destabilizing residue in the N-end rule (Fig. 1), is a physiological substrate of the N-end rule pathway (Fig. 2–5). In particular, the metabolic stability of LLO, in reticulocyte extract, in mouse NIH 3T3 cells, and in the cytosol of infected mouse cells, depended on the identity of the N-terminal residue of LLO, with stabilizing residues, such as Gly and Val, strongly inhibiting LLO degradation (see Results).

The N-end rule pathway is a Ub-dependent proteolytic pathway that is present in all eukaryotes examined (Fig. 1 shows the pathway's diagram; see also the introduction). Replacing the N-terminal Lys of LLO with a stabilizing residue such as Val increased the in vivo half-life of LLO but did not strongly affect the intracellular growth or virulence of *L. monocytogenes*. This finding suggests that the rapid degradation of LLO by the N-end rule pathway is not a primary mechanism to control LLO activity in the host cytosol. However, our previous work has shown that a combination of pharmacological inhibition of the proteasome-dependent degradation of LLO and a mutation in LLO that increases the rate of its synthesis is synergistically cytotoxic to infected mouse cells, implying that the in vivo degradation of secreted LLO is functionally relevant (53). In the present study, we also found that double mutant *L. monocytogenes* strains in which upregulated secretion of LLO was combined with the presence of a stabilizing residue (such as Gly or Val) at the LLO N terminus were synergistically and severely cytotoxic to infected mammalian cells, a property that
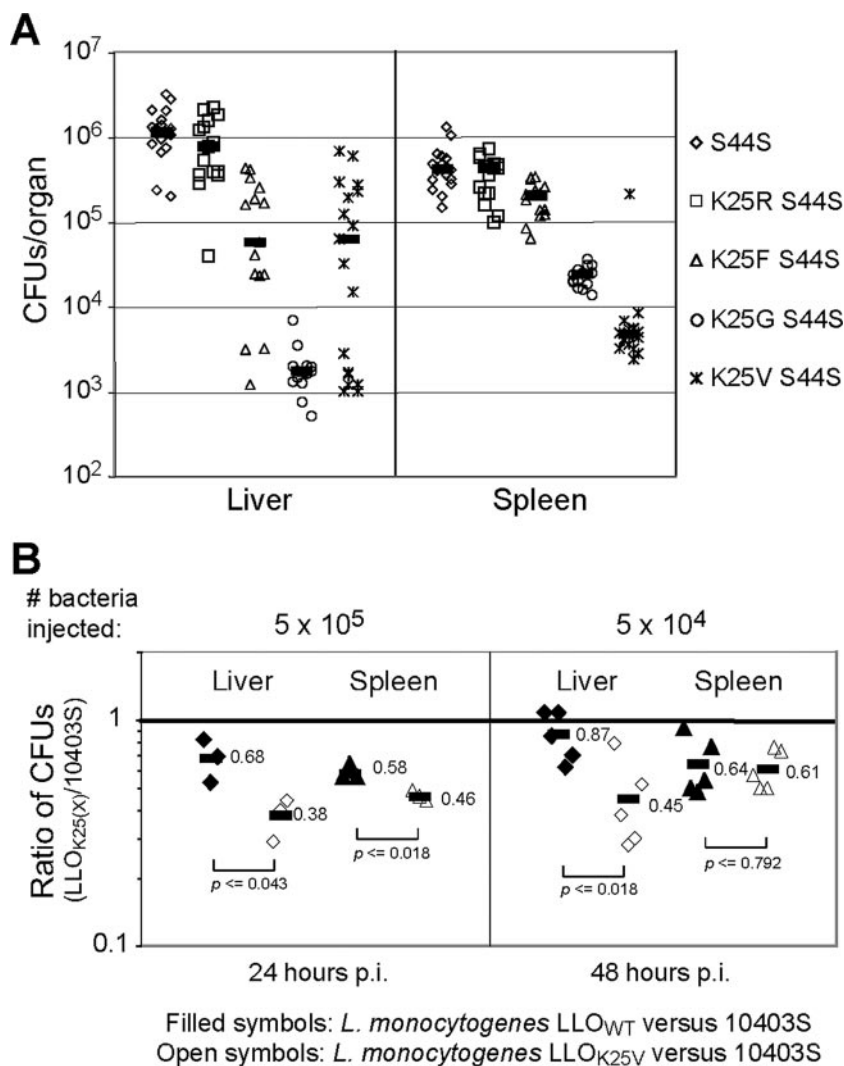
FIG. 7. Metabolic stabilization of LLO decreases the virulence of *L. monocytogenes* in mice. (A) BALB/c mice were inoculated, by tail vein injection, with 10^6 bacteria of the *L. monocytogenes* strains with the indicated mutations. All bacteria contained the LLO S44S mutation that results in the overproduction of LLO and, in addition, either the wild-type N-terminal Lys residue of LLO or its replacement residue, as shown. CFU were recovered from the livers and spleens 24 h postinoculation by plating dilutions of organ homogenates onto LB plates. Values shown represent the pooled data from at least three independent experiments, with five mice per strain of *L. monocytogenes*. Black horizontal bars indicate median values for each data set. (B) Competitive indices of *L. monocytogenes* 10403S versus the complemented *hly* deletion strains expressing either wild-type LLO or LLO$_{K25V}$. A 1:1 mixture of complemented Δ*hly L. monocytogenes* and wild-type 10403S *L. monocytogenes* was coinjected into the tail veins of BALB/c mice. The ratio of each strain in the livers and spleens was determined by plating organ homogenates and subsequently screening 100 colonies for the chloramphenicol resistance phenotype of the complemented strain. The *P* values indicated were obtained with Student's *t* test for two samples (http://www.statpages.org).

reduced the ability of the bacteria to grow intracellularly and resulted in a ~100-fold decrease in virulence. Thus, the degradation of LLO by the N-end rule pathway can, in principle, function as a backup mechanism to control the pore-forming activity of LLO and to protect the intracellular niche of *L. monocytogenes* when LLO is overproduced during the cytosolic growth of *L. monocytogenes*.

The secretion of specific protein effectors into the cytosol of eukaryotic host cells is a widespread strategy of bacterial pathogens. These bacterial effectors are important virulence factors that can perturb a wide variety of host processes such as phagocytosis, apoptosis, vesicular trafficking, and the innate immune response to infection (8, 17, 21, 42). The role and

importance of the host's degradative machinery in the control of the function of these microbial effectors are becoming increasingly clear (3). For example, the invasion of epithelial cells by *Salmonella enterica* serovar Typhimurium requires the reversible activation of host Rho family GTPases by the bacterial guanine nucleotide exchange factor SopE and the GTPase-activating protein Spt. To temporally regulate their opposing functions, these two proteins utilize different rates of degradation by host proteasomes (35). Another type III effector recently identified to be ubiquitylated and degraded by the host proteasome pathway is the GTPase-activating protein YopE from *Yersinia enterocolitica* (50). The stabilization of YopE by the pharmacological inhibition of host proteasomes

led to an increase in the activity of its target GTPase, Rac, and a cytotoxic effect of YopE on the host cell (50).

A cytolysin such as LLO faces conflicting design specifications in its metabolic stability and other properties. For example, the secreted LLO should be able to form pores in the membrane of a macrophage's phagosome, thereby making possible the escape of *L. monocytogenes* into the cytosol. However, once the bacterium finds itself in the cytosol, excessive activity of secreted LLO would lead to pores in the plasma membrane, an alteration that can be directly cytotoxic to the host cell, resulting in the loss of the protective intracellular niche and the exposure of the bacteria to the hostile environment of the extracellular milieu. To balance these (and other) conflicting requirements, the evolutionary pressures that yielded the current *L. monocytogenes* LLO have made it much more active at the relatively low pH of phagosomes than at the near-neutral pH of the cytosol (25, 54). LLO is also a short-lived protein in the cytosol, being targeted, as shown in the present study, by the N-end rule pathway. The rates of synthesis and secretion of LLO by *L. monocytogenes* are also regulated by the bacterium's specific environment in ways that are still largely unexplored (10, 14, 52, 55).

Our demonstration that the (mutational) stabilization of LLO against targeting by the N-end rule pathway does not, by itself, have strong effects on physiological aspects of the growth and virulence of *L. monocytogenes* raises the question of how this regulatory mechanism is maintained. It should be noted that although the replacement of the N-terminal Lys residue of LLO with a stabilizing residue such as Val did not strongly affect the intracellular growth or virulence of *L. monocytogenes*, this replacement did decrease the virulence of *L. monocytogenes* by nearly twofold (Fig. 7B), suggesting that a destabilizing N-terminal residue of LLO may stem from positive selection during the evolution of this and related bacteria. Long-term evolutionary selection usually operates on marginal differences in fitness. In other words, it is possible, indeed likely, that the relative smallness of the physiological effects that result from the metabolic stabilization of LLO and the short-term nature of laboratory-based tests may not suffice to detect the evolutionary relevance of such effects under conditions of long-term selection of bacteria in their natural habitats. Thus, moderate (even weak) but long-term selection pressures may account, at least in part, for the observed degradation of the secreted *L. monocytogenes* LLO by the N-end rule pathway.

The physiological significance of LLO degradation may also vary for different *L. monocytogenes* strains. The N-terminal Lys residue of LLO, a primary destabilizing residue in the N-end rule (Fig. 1), is conserved in the ~150 quasi-independent isolates of *L. monocytogenes* in which the LLO-encoding gene *hly* has been sequenced (P. Schnupf and D. A. Portnoy, unpublished data). In addition, the predicted N-terminal Asp residue of secreted ivanolysin O, an LLO-like cytolysin from pathogenic *L. ivanovii*, is also a destabilizing residue in the N-end rule (Fig. 1). However, 63% of the *hly* sequences displayed changes in more than 40 nucleotides compared to the *hly* sequence of our wild-type *L. monocytogenes* strain 10403S (as well as that of the other commonly used wild-type strain, EGD-e). Furthermore, more than 50% of the available *hly* sequences displayed between one and six nucleotide changes compared to

the wild-type sequences within the first 52 codons, a region previously shown to restrict the translation of LLO during the cytosolic growth of *L. monocytogenes* (52). These nucleotide changes were predominantly in codons 14, 18, 19, 26, 31, 35, and 39 (and combinations thereof). Because a nucleotide change in codon 44 can result in a dramatic increase in LLO production during the cytosolic growth of *L. monocytogenes* and a severe virulence defect (24, 52, 53), the identified sequence divergence within the 5′ region of *hly* among the clinical isolates may contribute to differences in the translational control and hence the production of LLO during the cytosolic growth of the bacteria. Alternatively, because many of the nucleotide changes also resulted in amino acid changes, strain differences in the LLO protein may affect the pH optimum and/or protein-protein interactions that may keep LLO inactive in the host cytosol. Thus, strain variations in the production and the activity of the LLO protein are two other possible means by which selective pressure for LLO degradation may be maintained.

One functionally relevant aspect of the metabolic instability of LLO is that the immunodominant LLO peptide comprising residues 91 to 99 (peptide 91-99) becomes presented on major histocompatibility complex class I molecules on the surfaces of infected cells, where it is recognized by cytotoxic T cells (19). When host proteasomes are inhibited, the presentation of LLO peptide 91-99 is blocked (67, 68). While it is still unknown whether the in vivo half-life of secreted LLO influences the presentation of LLO peptide 91-99, it was previously shown that the proteasome-dependent degradation of another secreted *L. monocytogenes* protein, called p60 (a cell wall hydrolase and a prominent antigen of *L. monocytogenes*), facilitates the presentation of its major histocompatibility complex class I epitope (57).

It should be noted that the secreted p60 protein, which bears N-terminal Ser and has a moderately short in vivo half-life of ~75 min (57), is not a substrate of the N-end rule pathway as it is understood at present (Fig. 1). The same is true for ActA, another secreted *L. monocytogenes* protein, which bears N-terminal Ala (40). While early work (26) indicated that otherwise-identical reporter proteins bearing N-terminal Ala, Ser, and Thr residues were shorter lived than those bearing stabilizing N-terminal residues such as Gly and Val, subsequent attempts to identify an E3 Ub ligase(s) that recognizes the above-mentioned N-terminal residues have not been successful thus far. In addition, the N-terminal Ala, Ser, and Thr are acetylated in many proteins that bear such residues, further complicating the disposition. Both ActA and p60 can be made much shorter lived than their wild-type counterparts by converting their N-terminal Ala and Ser, respectively, into destabilizing residues of the currently known N-end rule pathway (Fig. 1) (40, 57). However, for the reasons given above, that fact by itself is insufficient for concluding, as yet, that the in vivo degradation of wild-type ActA and p60 involves the specific recognition of their N-terminal residues by a (presumed) E3 Ub ligase(s). The secreted LLO protein which bears N-terminal Lys, a type 1 destabilizing residue (Fig. 1), is thus, at present, the sole bona fide N-end rule substrate among the secreted proteins of *L. monocytogenes*.

In summary, the pore-forming activity of LLO must be tightly regulated to prevent host cell lysis during cytosolic

growth (16, 24, 25, 52). Two previously described posttranscriptional mechanisms that limit LLO-mediated toxicity to the host cell are the control of LLO synthesis in the host cell cytosol by the negative regulation of LLO translation (52) and the decreased activity of LLO at the neutral pH of the cytosol (a low-pH optimum of LLO) (25). As shown above, the degradation of LLO by the host's N-end rule pathway is yet another postranscriptional mechanism of LLO regulation that can limit LLO-mediated toxicity and may have been selected for its positive effects on fitness during the evolution of *L. monocytogenes*.

ACKNOWLEDGMENTS

REFERENCES

1. **Alouf, J. E.** 2001. Pore-forming bacterial protein toxins: an overview. Curr. Top. Microbiol. Immunol. **257**:1–14.
2. **An, J. Y., J. W. Seo, T. Tasaki, M. J. Lee, A. Varshavsky, and Y. T. Kwon.** 2006. Impaired neurogenesis and cardiovascular development in mice lacking the E3 ubiquitin ligases UBR1 and UBR2 of the N-end rule pathway. Proc. Natl. Acad. Sci. USA **103**:6212–6217.
3. **Angot, A., A. Vergunst, S. Genin, and N. Peeters.** 2007. Exploitation of eukaryotic ubiquitin signaling pathways by effectors translocated by bacterial type III and type IV secretion systems. PLoS Pathog. **3**:e3.
4. **Ardley, H. C., and P. A. Robinson.** 2005. E3 ubiquitin ligases. Essays Biochem. **41**:15–30.
5. **Auerbuch, V., L. Lenz, and D. A. Portnoy.** 2001. Development of a competitive index assay to evaluate the virulence of *Listeria monocytogenes actA* mutants during primary and secondary infection of mice. Infect. Immun. **69**:5953–5957.
6. **Ausubel, F. M., R. Brent, R. E. Kingston, D. D. Moore, J. A. Smith, J. G. Seidman, and K. Struhl.** 2002. Current protocols in molecular biology. Wiley-Interscience, New York, NY.
7. **Bachmair, A., and A. Varshavsky.** 1989. The degradation signal in a short-lived protein. Cell **56**:1019–1032.
8. **Backert, S., and T. F. Meyer.** 2006. Type IV secretion systems and their effectors in bacterial pathogenesis. Curr. Opin. Microbiol. **9**:207–217.
9. **Baker, R. T., and A. Varshavsky.** 1991. Inhibition of the N-end rule pathway in living cells. Proc. Natl. Acad. Sci. USA **87**:2374–2378.
10. **Behari, J., and P. Youngman.** 1998. Regulation of *hly* expression in *Listeria monocytogenes* by carbon sources and pH occurs through separate mechanisms mediated by PrfA. Infect. Immun. **66**:3635–3642.
11. **Bishop, D. K., and D. J. Hinrichs.** 1987. Adoptive transfer of immunity to Listeria monocytogenes. The influence of in vitro stimulation on lymphocyte subset requirements. J. Immunol. **139**:2005–2009.
12. **Brundage, R. A., G. A. Smith, A. Camilli, J. A. Theriot, and D. A. Portnoy.** 1993. Expression and phosphorylation of the Listeria monocytogenes ActA protein in mammalian cells. Proc. Natl. Acad. Sci. USA **90**:11890–11894.
13. **Cardozo, T., and M. Pagano.** 2004. The SCF ubiquitin ligase: insights into a molecular machine. Nat. Rev. Mol. Cell. Biol. **5**:739–751.
14. **Datta, A. R., and M. H. Kothary.** 1993. Effects of glucose, growth temperature, and pH on listeriolysin O production in *Listeria monocytogenes*. Appl. Environ. Microbiol. **59**:3495–3497.
15. **Davydov, I. V., and A. Varshavsky.** 2000. RGS4 is arginylated and degraded by the N-end rule pathway in vitro. J. Biol. Chem. **275**:22931–22941.
16. **Decatur, A. L., and D. A. Portnoy.** 2000. A PEST-like sequence in listeriolysin O essential for Listeria monocytogenes pathogenicity. Science **290**:992–995.
17. **Desvaux, M., and M. Hebraud.** 2006. The protein secretion systems in Listeria: inside out bacterial virulence. FEMS Microbiol. Rev. **30**:774–805.
18. **Domann, E., J. Wehland, M. Rohde, S. Pistor, M. Hartl, W. Goebel, M. Leimeister-Wachter, M. Wuenscher, and T. Chakraborty.** 1992. A novel bacterial virulence gene in Listeria monocytogenes required for host cell microfilament interaction with homology to the proline-rich region of vinculin. EMBO J. **11**:1981–1990.

19. **Finelli, A., K. M. Kerksiek, S. E. Allen, N. Marshall, R. Mercado, I. Pilip, D. H. Busch, and E. G. Pamer.** 1999. MHC class I restricted T cell responses to *Listeria monocytogenes*, an intracellular bacterial pathogen. Immunol. Res. **19**:211–223.
20. **Gaillard, J. L., P. Berche, and P. Sansonetti.** 1986. Transposon mutagenesis as a tool to study the role of hemolysin in the virulence of *Listeria monocytogenes*. Infect. Immun. **52**:50–55.
21. **Galan, J. E.** 2001. Salmonella interactions with host cells: type III secretion at work. Annu. Rev. Cell Dev. Biol. **17**:53–86.
22. **Gardner, R. G., and R. Y. Hampton.** 1999. A "distributed degron" allows regulated entry into the ER degradation pathway. EMBO J. **18**:5994–6004.
23. **Gedde, M. M., D. E. Higgins, and D. A. Portnoy.** 2000. Role of listeriolysin O in cell-to-cell spread of *Listeria monocytogenes*. Infect. Immun. **68**:999–1003.
24. **Glomski, I. J., A. L. Decatur, and D. A. Portnoy.** 2003. *Listeria monocytogenes* mutants that fail to compartmentalize listeriolysin O activity are cytotoxic, avirulent, and unable to evade host extracellular defenses. Infect. Immun. **71**:6754–6765.
25. **Glomski, I. J., M. M. Gedde, A. W. Tsang, J. A. Swanson, and D. A. Portnoy.** 2002. The Listeria monocytogenes hemolysin has an acidic pH optimum to compartmentalize activity and prevent damage to infected host cells. J. Cell Biol. **156**:1029–1038.
26. **Gonda, D. K., A. Bachmair, I. Wünning, J. W. Tobias, W. S. Lane, and A. Varshavsky.** 1989. Universality and structure of the N-end rule. J. Biol. Chem. **264**:16700–16712.
27. **Groll, M., M. Bochtler, H. Brandstetter, T. Clausen, and R. Huber.** 2005. Molecular machines for protein degradation. Chembiochem **6**:222–256.
28. **Hershko, A., A. Ciechanover, and A. Varshavsky.** 2000. The ubiquitin system. Nat. Med. **10**:1073–1081.
29. **Hu, R.-G., C. S. Brower, H. Wang, I. V. Davydov, J. Sheng, J. Zhou, Y. T. Kwon, and A. Varshavsky.** 2006. Arginyl-transferase, its specificity, putative substrates, bidirectional promoter, and splicing-derived isoforms. J. Biol. Chem. **281**:32559–32573.
30. **Hu, R.-G., J. Sheng, Q. Xin, Z. Xu, T. T. Takahashi, and A. Varshavsky.** 2005. The N-end rule pathway as a nitric oxide sensor controlling the levels of multiple regulators. Nature **437**:981–986.
31. **Johnson, E. S., D. K. Gonda, and A. Varshavsky.** 1990. *cis-trans* recognition and subunit-specific degradation of short-lived proteins. Nature **346**:287–291.
32. **Jones, S., and D. A. Portnoy.** 1994. Characterization of *Listeria monocytogenes* pathogenesis in a strain expressing perfringolysin O in place of listeriolysin O. Infect. Immun. **62**:5608–5613.
33. **Kathariou, S., P. Metz, H. Hof, and W. Goebel.** 1987. Tn916-induced mutations in the hemolysin determinant affecting virulence of *Listeria monocytogenes*. J. Bacteriol. **169**:1291–1297.
34. **Kocks, C., E. Gouin, et al.** 1992. L. monocytogenes-induced actin assembly requires the actA gene product, a surface protein. Cell **68**:521–531.
35. **Kubori, T., and J. E. Galan.** 2003. Temporal regulation of salmonella virulence effector function by proteasome-dependent protein degradation. Cell **115**:333–342.
36. **Kwon, Y. T., A. S. Kashina, I. V. Davydov, R.-G. Hu, J. Y. An, J. W. Seo, F. Du, and A. Varshavsky.** 2002. An essential role of N-terminal arginylation in cardiovascular development. Science **297**:96–99.
37. **Kwon, Y. T., Z. X. Xia, J. Y. An, T. Tasaki, I. V. Davydov, J. W. Seo, Y. Xie, and A. Varshavsky.** 2003. Female lethality and apoptosis of spermatocytes in mice lacking the UBR2 ubiquitin ligase of the N-end rule pathway. Mol. Cell. Biol. **23**:8255–8271.
38. **Lauer, P., M. Y. Chow, M. J. Loessner, D. A. Portnoy, and R. Calendar.** 2002. Construction, characterization, and use of two *Listeria monocytogenes* site-specific phage integration vectors. J. Bacteriol. **184**:4177–4186.
39. **Lévy, F., N. Johnsson, T. Rümenapf, and A. Varshavsky.** 1996. Using ubiquitin to follow the metabolic fate of a protein. Proc. Natl. Acad. Sci. USA **93**:4907–4912.
40. **Moors, M. A., V. Auerbuch, and D. A. Portnoy.** 1999. Stability of the Listeria monocytogenes ActA protein in mammalian cells is regulated by the N-end rule pathway. Cell. Microbiol. **1**:249–257.
41. **Moors, M. A., B. Levitt, P. Youngman, and D. A. Portnoy.** 1999. Expression of listeriolysin O and ActA by intracellular and extracellular *Listeria monocytogenes*. Infect. Immun. **67**:131–139.
42. **Mota, L. J., I. Sorg, and G. R. Cornelis.** 2005. Type III secretion: the bacteria-eukaryotic cell express. FEMS Microbiol. Lett. **252**:1–10.
43. **Nato, F., K. Reich, S. Lhopital, C. Geoffroy, J. C. Mazie, and P. Cossart.** 1991. Production and characterization of neutralizing and nonneutralizing monoclonal antibodies against listeriolysin O. Infect. Immun. **59**:4641–4646.
44. **Pickart, C.** 2004. Back to the future with ubiquitin. Cell **116**:181–190.
45. **Portnoy, D. A., T. Chakraborty, W. Goebel, and P. Cossart.** 1992. Molecular determinants of *Listeria monocytogenes* pathogenesis. Infect. Immun. **60**:1263–1267.
46. **Portnoy, D. A., P. S. Jacks, and D. J. Hinrichs.** 1988. Role of hemolysin for the intracellular growth of Listeria monocytogenes. J. Exp. Med. **167**:1459–1471.
47. **Prakash, S., L. Tian, K. S. Ratliff, R. E. Lehotzky, and A. Matouschek.** 2004.

An unstructured initiation site is required for efficient proteasome-mediated degradation. Nat. Struct. Mol. Biol. **11:**830–837.

48. **Reiss, Y., D. Kaim, and A. Hershko.** 1988. Specificity of binding of N-terminal residues of proteins to ubiquitin-protein ligase. Use of amino acid derivatives to characterize specific binding sites. J. Biol. Chem. **263:**2693–2698.

49. **Rossjohn, J., S. C. Feil, W. J. McKinstry, R. K. Tweten, and M. W. Parker.** 1997. Structure of a cholesterol-binding, thiol-activated cytolysin and a model of its membrane form. Cell **89:**685–692.

50. **Ruckdeschel, K., G. Pfaffinger, K. Trulzsch, G. Zenner, K. Richter, J. Heesemann, and M. Aepfelbacher.** 2006. The proteasome pathway destabilizes Yersinia outer protein E and represses its antihost cell activities. J. Immunol. **176:**6093–6102.

51. **Schlech, W. F., III.** 2000. Foodborne listeriosis. Clin. Infect. Dis. **31:**770–775.

52. **Schnupf, P., J. Hofmann, J. Norseen, I. J. Glomski, H. Schwarzstein, and A. L. Decatur.** 2006. Regulated translation of listeriolysin O controls virulence of Listeria monocytogenes. Mol. Microbiol. **61:**999–1012.

53. **Schnupf, P., D. A. Portnoy, and A. L. Decatur.** 2006. Phosphorylation, ubiquitination and degradation of listeriolysin O in mammalian cells: role of the PEST-like sequence. Cell. Microbiol. **8:**353–364.

54. **Schuerch, D. W., E. M. Wilson-Kubalek, and R. K. Tweten.** 2005. Molecular basis of listeriolysin O pH dependence. Proc. Natl. Acad. Sci. USA **102:**12537–12542.

55. **Shen, A., and D. E. Higgins.** 2005. The 5′ untranslated region-mediated enhancement of intracellular listeriolysin O production is required for Listeria monocytogenes pathogenicity. Mol. Microbiol. **57:**1460–1473.

56. **Sheng, J., A. Kumagai, W. G. Dunphy, and A. Varshavsky.** 2002. Dissection of c-MOS degron. EMBO J. **21:**6061–6071.

57. **Sijts, A. J., I. Pilip, and E. G. Pamer.** 1997. The Listeria monocytogenes-secreted p60 protein is an N-end rule substrate in the cytosol of infected cells. Implications for major histocompatibility complex class I antigen processing of bacterial proteins. J. Biol. Chem. **272:**19261–19268.

58. **Skoble, J., D. A. Portnoy, and M. D. Welch.** 2000. Three regions within ActA promote Arp2/3 complex-mediated actin nucleation and Listeria monocytogenes motility. J. Cell Biol. **150:**527–538.

59. **Sun, A. N., A. Camilli, and D. A. Portnoy.** 1990. Isolation of *Listeria monocytogenes* small-plaque mutants defective for intracellular growth and cell-to-cell spread. Infect. Immun. **58:**3770–3778.

60. **Suzuki, T., and A. Varshavsky.** 1999. Degradation signals in the lysine-asparagine sequence space. EMBO J. **18:**6017–6026.

61. **Tilney, L. G., and D. A. Portnoy.** 1989. Actin filaments and the growth, movement, and spread of the intracellular bacterial parasite, Listeria monocytogenes. J. Cell Biol. **109:**1597–1608.

62. **Tweten, R. K.** 2005. Cholesterol-dependent cytolysins, a family of versatile pore-forming toxins. Infect. Immun. **73:**6199–6209.

63. **Varshavsky, A.** 2006. The early history of the ubiquitin field. Protein Sci. **15:**647–654.

64. **Varshavsky, A.** 1996. The N-end rule: functions, mysteries, uses. Proc. Natl. Acad. Sci. USA **93:**12142–12149.

65. **Varshavsky, A.** 2005. Ubiquitin fusion technique and related methods. Methods Enzymol. **399:**777–799.

66. **Vazquez-Boland, J. A., M. Kuhn, P. Berche, T. Chakraborty, G. Dominguez-Bernal, W. Goebel, B. Gonzalez-Zorn, J. Wehland, and J. Kreft.** 2001. Listeria pathogenesis and molecular virulence determinants. Clin. Microbiol. Rev. **14:**584–640.

67. **Vijh, S., and E. G. Pamer.** 1997. Immunodominant and subdominant CTL responses to Listeria monocytogenes infection. J. Immunol. **158:**3366–3371.

68. **Villanueva, M. S., A. J. Sijts, and E. G. Pamer.** 1995. Listeriolysin is processed efficiently into an MHC class I-associated epitope in Listeria monocytogenes-infected cells. J. Immunol. **155:**5227–5233.

69. **Zwickl, P., W. Baumeister, and A. Steven.** 2000. Dis-assembly lines: the proteasome and related ATP-assisted proteases. Curr. Opin. Struct. Biol. **10:**242–250.

Editor: J. B. Bliska